Plant Physiology and Biochemistry 145 (2019) 10–20

Contents lists available at ScienceDirect

Plant Physiology and Biochemistry

journal homepage: www.elsevier.com/locate/plaphy

Research article

Differential protein analysis of *Heracleum moellendorffii* Hance seeds during stratification

F.H. Li*, P. Yu, C.H. Song, J.J. Wu, Y. Tian, X.F. Wu, X.W. Zhang, Y.M. Liu

College of Life Science, Northeast Agricultural University, No. 600 Changjiang Road, Xiangfang District, Harbin, 150030, Heilongjiang, China

ARTICLE INFO

Keywords:
Heracleum moellendorffii hance
Low-temperature stratification
TMT
Germination and dormancy
Proteomic analysis

ABSTRACT

Heracleum moellendorffii Hance is a medicinal vegetable species, and the seed dormancy of this species has caused many agricultural problems. One stratification technique involves alternating layers of seeds and substrate to allow post-ripening of dormant seeds under appropriate environmental conditions and to release dormancy. Non-stratified seeds (NS), cotyledon-stage-embryo seeds (CS) and germinated seeds (GS) represent key stages of *H. moellendorffii* seeds during stratification. To better understand the breaking of dormancy caused by stratification, tandem mass tag (TMT) mass spectrometry (MS)/MS was used to detect proteins among NS, CS and GS. A total of 876 proteins were identified, which were subjected to Gene Ontology (GO) and Kyoto Encyclopedia of Genes and Genomes (KEGG) analyses. The results showed that carbohydrate metabolic processes, responses to stress and ribosome biogenesis were the main biological processes. The changes in protein accumulation were validated by qRT-PCR. The results showed that starch, sucrose, pyruvate and fatty acid metabolism played significant roles and that the contents of stored substances were gradually degraded during stratification. This study provides a theoretical basis in terms of proteomics for exploring the post-ripening and germination of *H. moellendorffii* seeds.

1. Introduction

Heracleum moellendorffii Hance is a perennial herbaceous herb of the Umbelliferae family and belongs to *Heracleum* L., which is also known as mountain celery, short fruit celery and large-leaved celery. *H. moellendorffii* is a shade-tolerant plant species that grows in coniferous and broad-leaved mixed forests and on river and lake shores, grasslands, meadows, and hills with dark, humid habitats in eastern and northern China, North Korea, and Russia (Wu et al., 1994). *H. moellendorffii* is rich in nutrients, and whole plants can be used for the production of medicines. This species has medicinal value and exerts certain alleviating effects on rheumatoid arthritis, headaches, high blood pressure, high blood sugar and high cholesterol (Diao et al., 2010). With increasing demand for *H. moellendorffii* and the depletion of wild resources of this species, the development of *H. moellendorffii* cultivation is needed. However, *H. moellendorffii* seeds exhibit dormancy characteristics. After the seeds mature, dormancy persists for a long time, and the germination percentage is low under natural conditions, which makes large-scale artificial botanical cultivation of *H. moellendorffii* difficult.

There are many causes of seed dormancy, which can be divided into five types: physiological dormancy, morphological dormancy, morphological physiological dormancy, physical dormancy and composite dormancy (Wijayabandara et al., 2013). The seeds of *H. moellendorffii* have dormant properties, and their type of dormancy is morphological physiological. Low-temperature stratification is an effective method for breaking seed dormancy and has an important effect on seed enzyme activity and seed vigor (Bao and Zhang, 2011). Stratification can promote the metabolism of stored substances and can alter the cell membrane structure of seeds to accelerate dormancy release (Zhang and Jing, 2015). Stratification can also promote changes in endogenous hormones within seeds (Yang et al., 2008).

Proteins have physiological functions in biological organisms. Proteins are the direct embodiment of life and are the ultimate performers of physiological functions. A gene transmits genetic information, but one gene may correspond to multiple proteins (Simpson and Dorow, 2001). In addition, different posttranslational modifications can occur after protein synthesis; therefore, biological activities need to be studied at the protein level. With the continuous development of high-throughput sequencing technology and bioinformatics, it is becoming increasingly common to study proteomic function at different time points and in different localities. Proteins regulate internal biochemical reactions and metabolic processes in seeds and play extremely important roles in the formation of mature plants, including roles in seed

* Corresponding author.
E-mail address: 18846075952@163.com (F.H. Li).

https://doi.org/10.1016/j.plaphy.2019.10.002
Received 13 May 2019; Received in revised form 16 September 2019; Accepted 1 October 2019
Available online 10 October 2019

development, germination and seedling formation. Proteomic changes during seed germination have been studied in *Prunus campanulata* Maxim (Chung-Shu et al., 2010), *Magnolia sieboldii* K. Koch (Lu et al., 2016), *Araucaria angustifolia* (Balbuena et al., 2011), and Norway maple (Pawłowski., 2016). The identified proteins were shown to be involved in various processes, such as embryo growth, hormone signaling, transcription, protein storage, ATP accumulation and respiration. In recent years, research on *H. moellendorffii* has been mostly limited to the analysis of edible and medicinal ingredients (Wang et al., 2017), plant growth and seed development characteristics (Li et al., 2017b), and seed morphological changes under stratification (Li et al., 2017a). However, proteomic studies on the process of *H. moellendorffii* seed germination have not been reported.

Non-stratified seeds (NS), cotyledon-stage-embryo seeds (CS) and germinated seeds (GS) under 4 °C stratification were used as the experimental materials in this study. We investigated the ontogenetic changes in the embryos of these three different groups of *H. moellendorffii* seeds. We then compared the physiological and proteomic changes within the seeds. Physiological indexes included the contents of soluble sugars, soluble starch, soluble protein and crude fat. We also used tandem mass tag (TMT) mass spectrometry (MS)/MS to quantitatively screen the differentially accumulated proteins among the NS, CS and GS, and the results of the proteomic analysis were subsequently confirmed by qRT-PCR. Our results may provide a theoretical basis for further revealing the regulatory mechanism of *H. moellendorffii* seed germination.

2. Materials and methods

2.1. Materials and experimental design

The experimental materials included seeds harvested from 6-year-old *Heracleum moellendorffii* Hance plants. The seeds were collected from the experimental field of the Forest Botanical Garden of Heilongjiang Province (45° 30′-45° 40′ N, 126° 45′-126° 43′ E), which has a continental monsoon climate and is in the mid-temperate zone in Harbin, in August 2017. In this region, the annual average temperature is 3.5 °C, and the annual average rainfall is approximately 400–600 mm. The cultivated soil beneath *H. moellendorffii* was a medium-thick black soil (pH 6.8); the organic matter content was 50.64 g kg^{-1}, and the available N, P and K contents were 229.80, 9.45 and 180 mg kg^{-1}, respectively. The planting density of *H. moellendorffii* was 20 × 30 cm. Plump seeds were sterilized with 75% ethanol for 30 s and then soaked in distilled water for 6 h. The treated seeds and clean sand were mixed together at a ratio of 2:3 and then placed into plastic boxes (whose length, width, and height were 19 cm, 13 cm and 11 cm, respectively). The seeds were then transferred to a 4 °C box for stratification. Non-stratified seeds (NS), cotyledon stage embryo seeds (CS) and germinated seeds (GS) were collected as experimental materials at 0 d, 90 d and 150 d during the 4 °C stratification, respectively. Three independent biological replicates of seeds were collected and stored at −80 °C after being frozen in liquid nitrogen.

2.2. Morphological observations and index measurements of the seeds

2.2.1. Morphological observations

The seed coat was removed, and the endosperm length was measured with a Vernier caliper. A scalpel was used to remove the embryos to make a temporary loading. Under a microscope (Motic B1 Series), the embryo length was measured with a linear micrometer in conjunction with photomicrography. The measurement was repeated 10 times, and the average value was used to calculate the embryo rate. The measurement criteria were as follows:

Endosperm length: a Vernier caliper was used to measure the maximum length of the endosperm;

Embryo length: a linear micrometer was used to measure the maximum length of the embryo;

Embryo rate = embryo length / endosperm length × 100%

2.2.2. Measurement of physiological and biochemical indexes

Soluble sugar and starch contents were determined according to a anthrone method (Laurentin, 2003). The soluble protein content was determined according to a method involving Coomassie brilliant blue G250, and the crude fat content was determined according to a Soxhlet extraction method (Tang, 1999).

2.3. Protein preparation and protein extraction

Different samples (NS, CS and GS) were placed into a mortar precooled in liquid nitrogen. The samples were then ground in liquid nitrogen until the tissue completely formed a white powder. The ground powder was subsequently transferred to a 5 mL centrifuge tube, which was placed on ice, after which the mixture was homogenized for 15 min in lysis buffer (8 M urea, 30 mM hydroxyethyl piperazineethanesulfonic acid [HEPES], 1 mM phenylmethylsulfonyl fluoride [PMSF], 2 mM EDTA, and 10 mM dithiothreitol [DTT]). After homogenization, the solution was placed into an Eppendorf (EP) tube, which was then centrifuged at 20,000 g for 30 min at 4 °C. Prechilled acetone was then added to the supernatant, which was precipitated for 3 h at −20 °C; the amount of acetone was 4 times that of the supernatant. The mixed solution was subsequently centrifuged at 20,000 g for 30 min at 4 °C, after which the supernatants were discarded. Lysate was then added to the precipitate (8 M urea, 30 mM HEPES, 1 mM PMSF, 2 mM EDTA, and 10 mM DTT), and the samples were ultrasonicated for 5 min at 180 W for solubilization. Afterward, DTT was added to the samples such that the final concentration was 10 mM, after which the samples were incubated at 56 °C for 1 h. Iodoacetamide was then added to the samples such that the final concentration was 55 mM, after which the samples were incubated in the dark for 1 h. Last, the samples were centrifuged at 20,000 g for 30 min at 4 °C, after which the supernatant was collected. The protein concentration then determined via the Coomassie brilliant blue G250 method.

2.4. Enzymatic hydrolysis of protein

A total of 100 μg of protein was taken from each sample and then centrifuged at 14,000 g for 40 min at 4 °C. The supernatants were subsequently discarded. Afterward, 200 μL (50 mM) of tetraethylammonium bromide (TEAB) was added to the precipitates, which were then centrifuged at 14,000 g for 40 min at 4 °C. The supernatants were then discarded. This step was repeated twice. Afterward, 3.3 μg (1 μg μL^{-1}) of enzyme was added to each 100 μg of protein, which was then incubated at 37 °C for 24 h. The digested material was lyophilized, after which 30 μL (100 mM) of TEAB was used to reconstitute the peptide.

2.5. Protein labeling

Forty-one microliters of acetonitrile were added to each labeling reagent, which were then vortexed for 1 min and centrifuged at 1000 g to mix the samples evenly. The peptide segments were added to the mixed labeling reagent, and different samples were labeled with different isotopes (131-labeled sample, NS-1; 130C-labeled sample, NS-2; 130N-labeled sample, NS-3; 129C-labeled sample, CS-1; 128C-labeled sample, CS-2; 128N-labeled sample, CS-3; 127C-labeled sample, GS-1; 127N-labeled sample, GS-2; and 126-labeled sample, GS-3). The reaction was terminated with 8 mL (5%) of hydroxylamine for 15 min. The samples were mixed and allowed to stand at room temperature for 1 h. The labeled samples were subsequently vacuum dried with a vacuum concentrator.

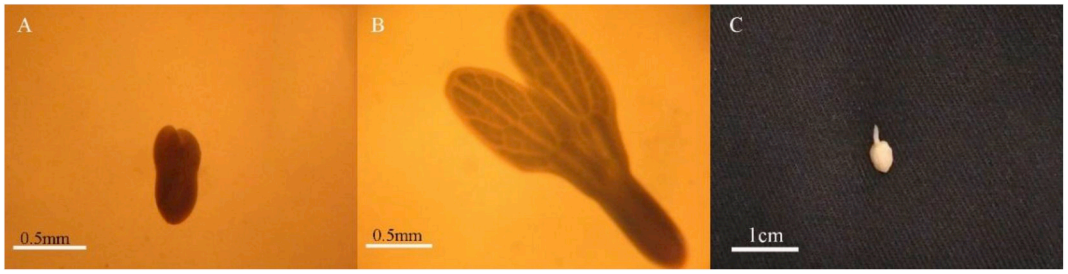

Fig. 1. Microstructure of seed embryos and a schematic chart of seed germination during low-temperature stratification. A, Heart-shaped-embryo stage; B, cotyledon-stage embryo; C, germinated seeds (GS).

Table 1
Basic information of the three stages of embryonic morphology.

	NS	CS	GS
Embryo length (mm)	0.69 ± 0.01Aa	2.24 ± 0.03Bb	–
Endosperm length (mm)	5.13 ± 0.06Cc	5.1 ± 0.05Cc	5.15 ± 0.02Cc
Embryo rate (%)	13.45 ± 0.27Dd	43.92 ± 0.89Ee	–
Bud length (mm)	–	–	3.01 ± 0.13Ff

Note: The different capital letters mean extremely significant differences at the 0.01 level, and the different lowercase letters mean significant differences at the 0.05 level. NS: nonstratified seeds; CS: cotyledon-stage-embryo seeds; GS: germinated seeds. The same scheme applies below.

2.6. Separation of peptide mixtures and MS

Desalted peptide mixtures were loaded onto an Acclaim PepMap C18-reversed-phase column (75 μm × 2 cm, 3 μM, 100 Å, Thermo Scientific) and separated on a reversed-phase C18 column (75 μM × 10 cm, 5 μM, 300 Å, Agela Technologies) mounted on a Dionex Ultimate 3000 Nano LC system. The peptides were eluted using a gradient of 5–80% (v/v) acetonitrile in 0.1% formic acid for 45 min at a flow rate of 300 nL min^{-1} combined with a Q-Exactive mass spectrometer (Thermo Fisher Scientific, MA, USA). The eluates were directly injected into the Q-Exactive mass spectrometer. The mass spectrometer was run in positive ion mode in a data-dependent manner with a full MS scan from 350-2000 m/z, a full-scan resolution of 70,000, and an MS/MS scan resolution of 35,000. The MS/MS scan was run with a minimum signal threshold of 1E + 5 and an isolation width of 2 Da. To evaluate the performance of the analysis of this mass spectrometer on the TMT-labeled samples, two MS/MS acquisition modes and higher collision energy dissociation (HCD) were used. To optimize the MS/MS acquisition efficiency of HCD, normalized collision energy (NCE) was systemically examined at 28 steps of 20%.

2.7. Validation of protein accumulation by qRT-PCR

Total RNA was extracted from the *H. moellendorffii* seeds with TRIzol (Takara) and DNase I treatment. The total RNA was reverse transcribed into first-strand cDNA using reverse-transcription enzymes, after which genes corresponding to differential proteins were selected. PCR was performed in a 20 μL reaction mixture containing 2 × SYBR Premix Ex Taq (Takara, China), 0.4 μL of each PCR primer (10 mmol. L^{-1}), 0.4 μL of 50 × ROX reference dye, and approximately 30 ng of cDNA per sample. The PCR conditions were as follows: 95 °C for 30 s, followed by 40 cycles of 95 °C for 5 s and 60 °C for 34 s. Three independent biological replicates were performed for each treatment. Dissociation curves were generated for each reaction to ensure specific amplification. The *Actin* and *5.8S* genes of *H. moellendorffii* seeds were used as internal controls (Liu et al., 2018; Campos et al., 2015). The relative expression levels of the genes were calculated by the $2^{-\Delta\Delta Ct}$ method (Li et al., 2016). The sequences of the primer pairs are listed in Supplementary Table 1.

2.8. Database searches

Subcellular localization was predicted and analyzed via WoLF PSORT software. The Kyoto Encyclopedia of Genes and Genomes (KEGG) database (http://www.genome.jp/kegg/) was searched for metabolite pathways, and Gene Ontology (GO) (http://www.geneontology) was used for functional category analysis. GO and KEGG terms with adjusted p values < 0.05 were considered significantly enriched terms.

All assays were run in triplicate, and the data were analyzed with GraphPad Prism 7 and SPSS software. To reveal significant differences, the data were subjected to analyses of variance (ANOVAs), and the least significant difference (LSD) between the means was determined with Duncan's test.

3. Results

3.1. Morphological observations of seed embryos during stratification

To determine the time points at which dormancy was broken, seed samples were collected during low-temperature stratification. The ontogeny of the *H. moellendorffii* seed embryos was compared via microscopy. The results showed that the seed embryos continuously developed during 4 °C stratification (Fig. 1). Germinating seeds must first complete morphological and physiological post-ripening. The seed embryos of NS were mostly in the heart-shaped embryonic stage (Fig. 1A). The embryos changed from heart-shaped embryos to torpedo-shaped embryos to cotyledon-stage embryos, after which the whole process of embryonic development was complete (Fig. 1B). Finally, the radicle broke through the seed coat (Fig. 1C). The average embryo length of NS was only 0.69 mm. After approximately 90 d of 4 °C stratification, the embryos developed into cotyledon-stage embryos, and the average embryo length increased to 2.24 mm. Compared with that of NS, the average embryo length of CS increased 3.24-fold. The embryo rate of CS was significantly greater than that of NS. The embryo rates of NS and CS were 13.45% and 43.92%, respectively (Table 1).

3.2. Measurements of stored substances in seeds during stratification

To investigate the changes in stored substances within the endosperm during stratification, changes in soluble protein, soluble starch, soluble sugar and crude fat contents were analyzed. The contents of soluble protein, soluble starch, soluble sugars and crude fat in the NS were 644.60 mg g^{-1}, 19.74 mg g^{-1}, 174.83 mg g^{-1} and 8.20%, respectively; compared with those in NS, the stored substances in CS decreased by 26.84%, 71.86%, 22.72% and 35.75%, respectively, and compared with those in CS, the stored substances in GS decreased by 31.99%, 25.49%, 21.90% and 17.22%, respectively (Fig. 2). Therefore, the amount of stored substances within *H. moellendorffii* seeds during stratification tended to significantly decrease. Stored substances in the endosperm provide energy for embryo growth and promote the transition of seeds from dormancy to germination.

3.3. Functional identification and classification of proteins identified by TMT

To investigate the differences in protein accumulation among NS, CS and GS, samples were collected at 0, 90 and 150 d during stratification for TMT quantitative analysis, respectively. The proteins extracted from different samples were initially separated by one-dimensional SDS-PAGE to text integrity (Supplementary Fig. 1). A list of the mass peaks is shown in Supplementary Fig. 2A. A total of 302,470 spectra were obtained by a time-of-flight MS approach. Totals of 8807 unique spectra, 2122 peptides and 876 proteins were identified via the Mascot 2.3.02 search engine (Supplementary Fig. 2B). After enzymatic hydrolysis was performed, the length of the peptides was determined to be normally distributed and was mainly distributed within the range of 6–31 kDa (Supplementary Fig. 2C).

A total of 502 differentially accumulated proteins were obtained after the data were screened according to the following criteria: $p < 0.05$, ratio ≥ 1.2 or ratio ≤ 0.833. There were 86 differentially accumulated proteins in CS compared with NS, including 39 up-regulated proteins and 47 down-regulated proteins. A total of 278 differentially accumulated proteins were identified in GS compared with NS, 148 of which were up-regulated and 130 of which were down-regulated. A total of 414 differentially accumulated proteins were identified in GS compared with CS, 215 of which were up-regulated and 199 of which were down-regulated (Fig. 3A). It can be seen from the Venn diagram that there are 33 unique proteins during the transition from NS to CS, 361 protein accumulation changes during the transition from CS to GS, and 53 proteins whose accumulation changed throughout the entire stratification. These results differ only from those of the protein comparisons between GS and NS. The comparative study of the different stages helps us understand this process more clearly (Fig. 3B).

3.4. Functional annotation analysis of proteomic differences

3.4.1. Differentially accumulated protein analysis of enriched GO terms

GO categorization of the identified proteins was carried out to further categorize their functions. The detected proteins were annotated to 10 cellular components, 13 biological processes and 7 molecular functions (Fig. 4). Organelle (GO:0043,226) and membrane (GO:0016,020) were the most highly enriched cellular components, containing 57 and 14 proteins, respectively. Organelle proteins play an important role in cell structure and function, allowing cells to undergo normal metabolic activities. Cell membranes make the intracellular environment relatively stable, and membrane proteins help to exchange information, substances and energy with the surrounding environment. The most highly enriched biological process was cellular process (GO:0009987). There were 90 proteins involved in metabolic processes (GO:0008152), and there were 35 proteins involved in response to stimulus (GO:0050,896). The main molecular functions of these proteins were binding (GO:0005488) and catalytic activity (GO:0003824), involving 122 and 113 proteins, respectively.

The GO enrichment analysis revealed that 40 GO terms were significantly ($P \leq 0.05$) enriched. Heterocycle biosynthetic process (GO:0018,130), organic cyclic compound biosynthetic process (GO:1,901,362), and transporter activity (GO:0005215) were the significant

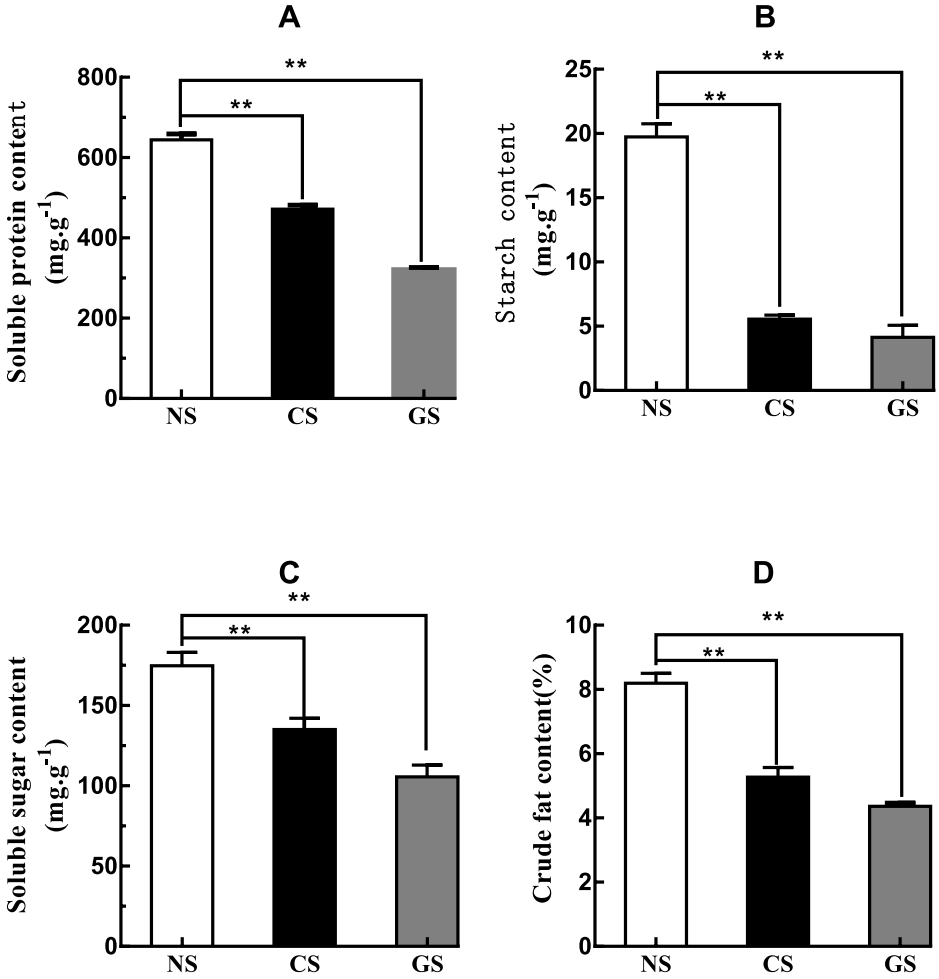

Fig. 2. Changes in the soluble protein (A), soluble starch (B), soluble sugar (C) and crude fat (D) contents within *H. moellendorffii* seeds among different stages. One-way analysis of variance (ANOVA) of data from cotyledon-stage-embryo seeds (CS) and germinated seeds (GS) compared with non-stratified seeds (NS). The asterisks indicate statistical significance, *P < 0.05, **P < 0.01. The error bars represent the means ± SEMs.

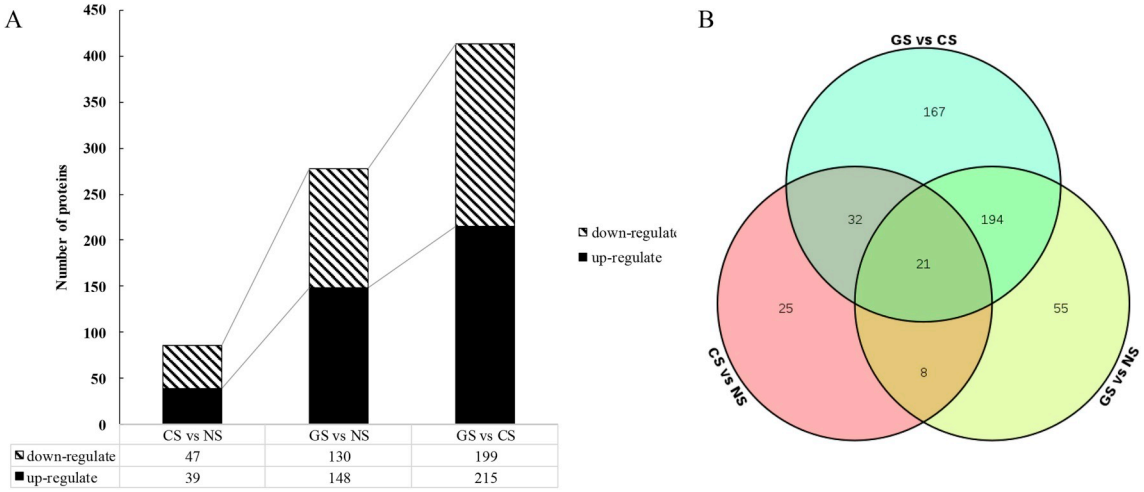

	CS vs NS	GS vs NS	GS vs CS
down-regulate	47	130	199
up-regulate	39	148	215

Fig. 3. Differentially accumulated proteins during stratification of *H. moellendorffii* seeds. Statistical analysis of differentially accumulated proteins (A). Venn diagram analysis of differentially accumulated proteins (B). NS, non-stratified seeds; CS, cotyledon-stage-embryo seeds; GS, germinated seeds.

terms in CS compared with NS. These proteins are mostly membrane proteins that play a role in mediating chemicals and signaling. Carbohydrate metabolic process (GO:0005975), small molecule catabolic process (GO:0044,282), response to stress (GO:0006950), carbohydrate derivative binding (GO:0097,367), organic cyclic compound binding (GO:0097,159) and heterocyclic compound binding (GO:1,901,363) were the significant terms in GS compared with NS. Protein metabolic process (GO:0019,538), response to stress (GO:0006950), and peptidase activity (GO:0070,011) were the significant terms in GS compared with CS (Supplementary Table 2).

Among these GO terms, 7 key proteins were identified, including Tubulin alpha chain (TUBA), Protein disulfide-isomerase (PDI), Heat shock 70 kDa protein (HSP70), elongation factor 1-beta (eEF1-β), Actin, FoF1-ATPase and L-ascorbate peroxidase (APX) (Supplementary Table 3). These proteins are related to protein metabolic processes and stress responses. Differences in GO entries and quantities of differentially enriched proteins occur at different stages.

3.4.2. Predictive analysis of the subcellular localization of differentially accumulated proteins

The subcellular localization of the identified proteins was predicted using WoLF PSORT software. The identified proteins were mainly

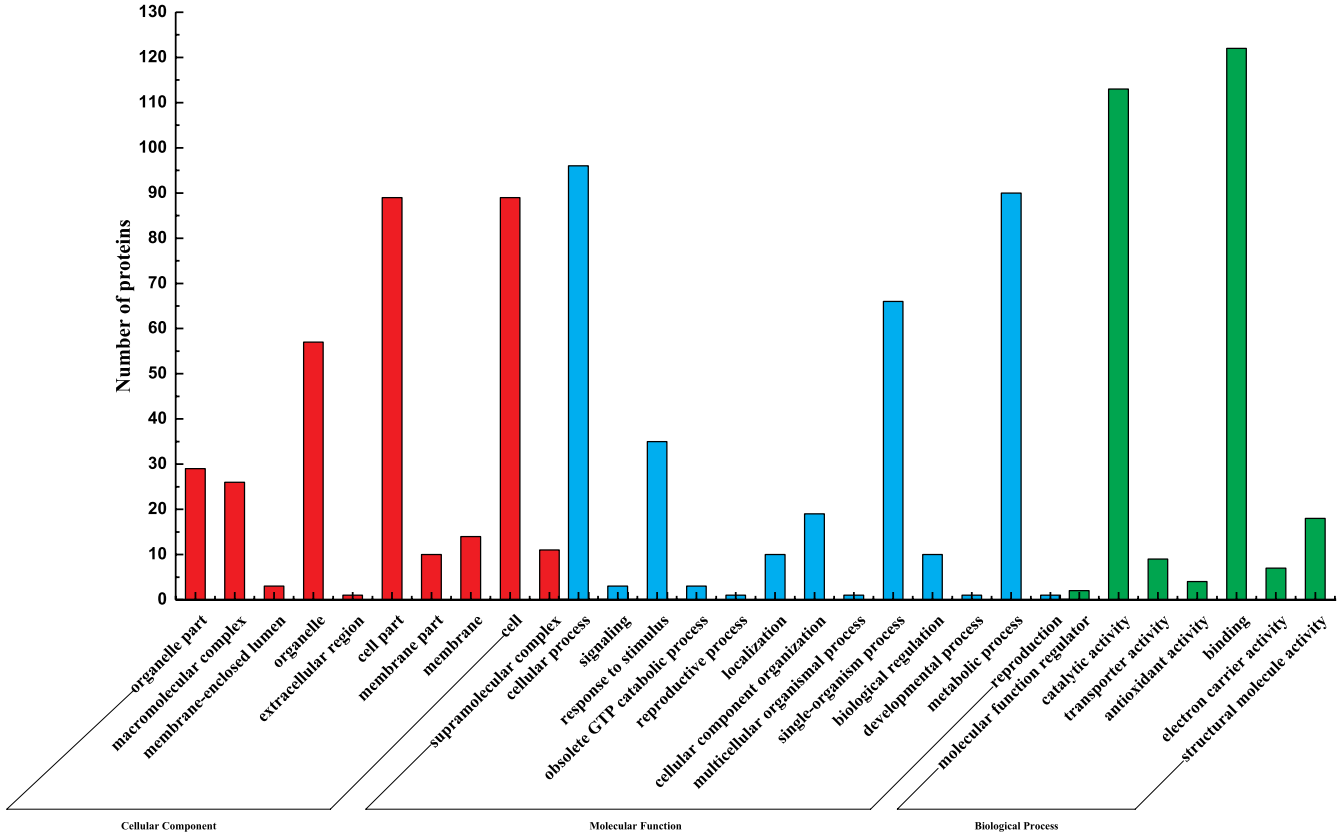

Fig. 4. GO functional classification of differentially accumulated proteins.

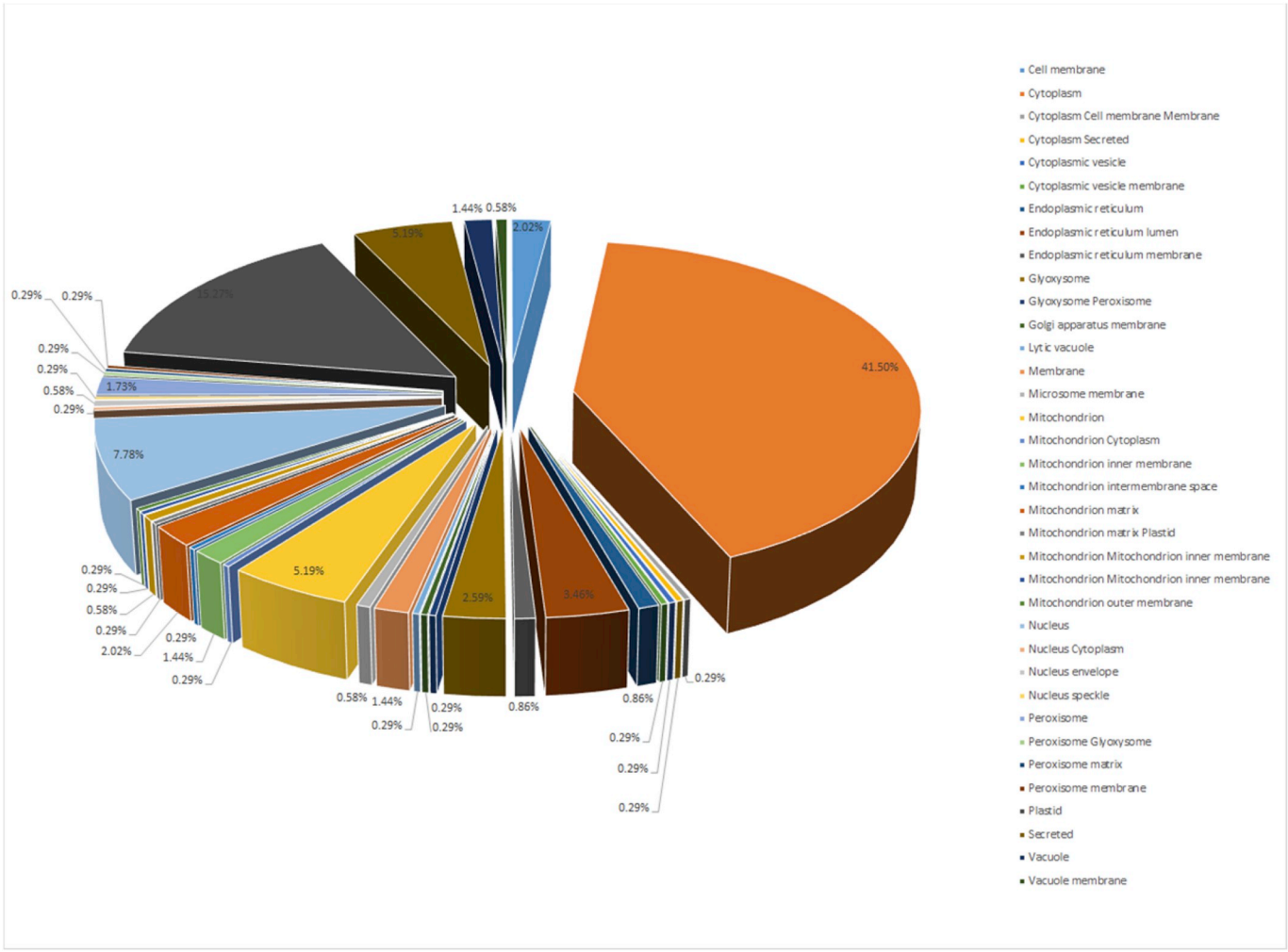

Fig. 5. Subcellular localization prediction of differentially accumulated proteins.

located in the cytoplasm (41.05%), plastid (15.27%), nucleus (7.78%), mitochondrion (5.19%), secreted (5.19%) and endoplasmic reticulum lumen (3.46%). Some proteins were also located in the peroxisome, glyoxysome, Golgi apparatus membrane, and lytic vacuole (Fig. 5). The results of this analysis provide a basis for further exploring the sites that function in the process of germination.

3.4.3. Differentially accumulated protein analysis of enriched KEGG terms

For KEGG enrichment, the differentially accumulated proteins were involved in a total of 108 metabolic pathways. The enriched metabolic pathways were identified by Fisher's exact test ($P < 0.05$). Ribosomes were significantly enriched in CS compared with NS. Five pathways were significantly enriched in GS compared with CS: those involving ribosomes, metabolic pathways, starch and sucrose metabolism, fatty acid degradation and fructose and mannose metabolism (Table 2). The pathways significantly enriched in GS compared with NS were the same as those in GS compared with CS. There were some differences in pathways in which seeds were significantly enriched during the 4 °C stratification. Various metabolic pathways in the cell provide energy and material protection for seed germination. Among them, the primary metabolic pathway accounts for the largest proportion.

Table 2
KEGG pathway enrichment analysis on the basis of the differentially accumulated proteins within *H. moellendorffii* seeds during stratification ($P < 0.05$).

Pathway_ acc	Description	p value		
		CS vs NS	GS vs NS	GS vs CS
map 04141	Protein processing in endoplasmic reticulum	> 0.05	0.0315	> 0.05
map 03010	Ribosome	0.0207	> 0.05	0.0086
map 01110	Biosynthesis of secondary metabolites	> 0.05	0.0089	> 0.05
map 01100	Metabolic pathways	> 0.05	4.3×10^{-6}	0.0061
map 00500	Starch and sucrose metabolism	> 0.05	> 0.05	0.0476
map 00450	Selenocompound metabolism	–	0.0146	> 0.05
map 00350	Tyrosine metabolism	> 0.05	0.0407	> 0.05
map 00270	Cysteine and methionine metabolism	> 0.05	0.0002	> 0.05
map 00071	Fatty acid degradation	> 0.05	> 0.05	0.0094
map 00051	Fructose and mannose metabolism	> 0.05	> 0.05	0.0303

3.5. Regulation of carbohydrate metabolism-related proteins during seed post-ripening

Carbohydrates are the main storage substances in seeds and are the main source of materials and energy for seed ripening and germination. A total of 116 proteins were involved in carbohydrate metabolism during 4 °C stratification. Among them, 62 differentially accumulated proteins were identified (Supplementary Table 4).

UTP-glucose-1-phosphate uridylyl transferase (UGP2, EC 2.7.7.9) is a key enzyme involved in starch synthesis. Compared with that in NS,

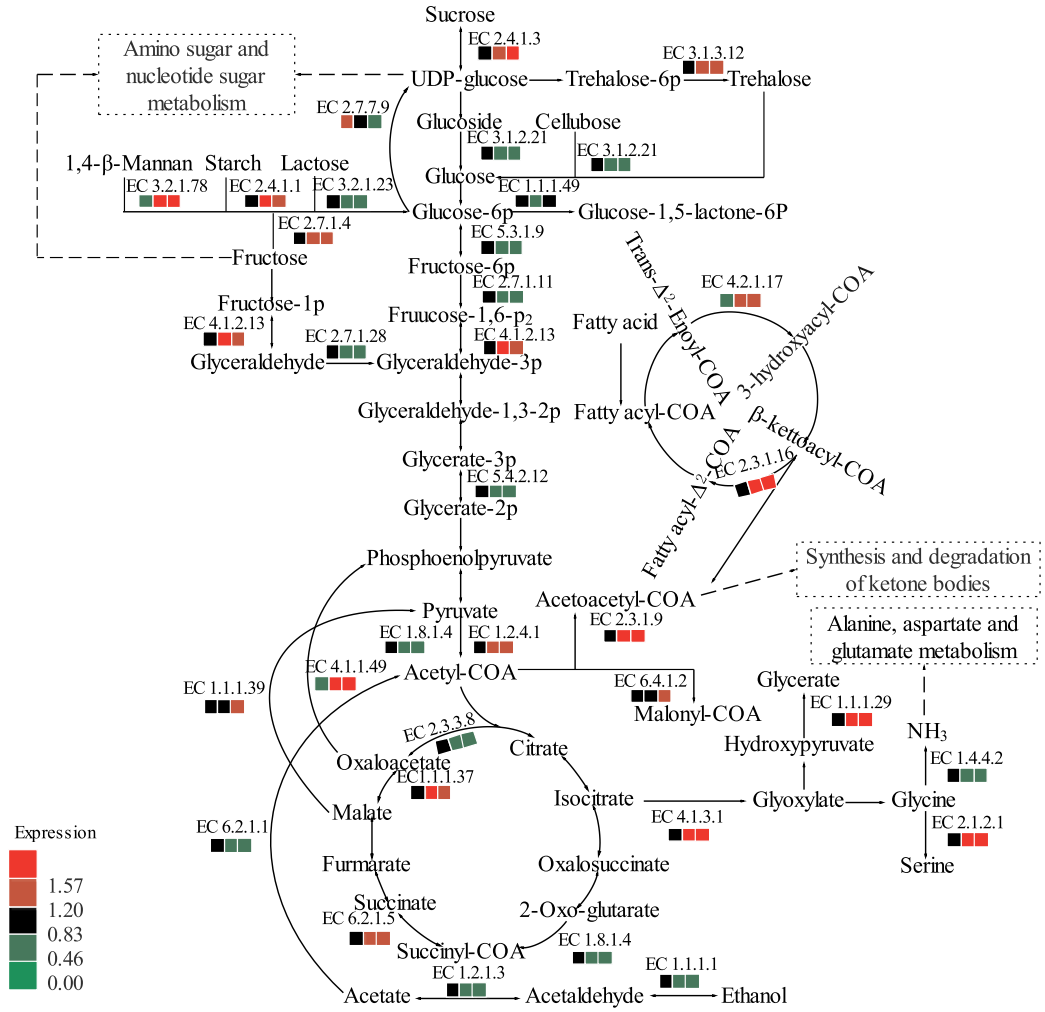

Fig. 6. Regulation of carbohydrate metabolism of *H. moellendorffii* seeds during post-ripening. Identified proteins detected in these pathways. The icons beside each protein name show the change in the protein level within the cotyledon-stage-embryo seeds (CS) and the germinated seeds (GS), with non-stratified seeds (NS) used as controls. Changes in proteins in GS, with CS used as controls.

the accumulation of this enzyme in CS was up-regulated but down-regulated in GS. Glycogen phosphorylase (PYG, EC 2.4.1.1) and trehalose 6-phosphate phosphatase (ostB, EC 3.1.3.12) are key enzymes involved in starch degradation; compared with that in NS, the accumulation of these enzymes in CS did not change significantly, but the accumulation of both proteins was up-regulated in GS. These findings indicate that starch catabolism was activated in the late stratification stage, which is consistent with the detected decrease in starch content.

Differentially accumulated proteins related to fructose, mannose and lactose metabolism were also identified, including dihydroxyacetone kinase (DAK, EC 2.7.1.28), fructokinase (scrK EC 2.7.1.4), mannan endo-1,4-beta-mannosidase (gmuG, EC 3.2.1.78), alpha-galactosidase (α-GLA, EC 3.2.1.22) and beta-galactosidase (β-GLA, EC 3.2.1.23). These differentially accumulated proteins are closely related to the soluble sugar content in seeds, which provides energy for seed germination through the glycolysis pathway (EMP), the tricarboxylic acid cycle (TCA) and the pentose phosphate pathway (PPP). Differentially accumulated proteins related to energy metabolism were also identified, among which the accumulation of xylose isomerase (EC 5.3.1.5) was significantly up-regulated in CS compared with NS. Xylose isomerase is an enzyme that is involved in EMP progression. The accumulation of proteins related to EMP and TCA, including fructose-bisphosphate aldolase (EC 4.1.2.13), phosphoenolpyruvate carboxykinase (EC 4.1.1.49), triosephosphate isomerase (EC 2.7.2.3), 2,3-bisphosphoglycerate-independent phosphoglycerate mutase (EC 2.7.1.90), dihydrolipoamide dehydrogenase (EC 1.8.1.4), the pyruvate dehydrogenase E1 component (EC 1.2.4.1), succinyl-CoA synthetase alpha subunit (EC 6.2.1.5) and malate dehydrogenase (MDH, EC 1.1.1.37), was significantly up-regulated in GS compared with CS. This result indicates that intraplant respiratory metabolism was activated, providing energy for the radicle to penetrate the seed coat. Pyruvic acid is one of the intermediates involved in the basic metabolism of entire organisms. Pyruvate is involved in the interconversion among sugars, fats and amino acids in biological organisms via acetyl-CoA and the TCA. The present results showed that enzymes involved in pyruvate metabolism, including orthophosphate dikinase (EC 2.7.9.1) and acetyl-CoA carboxylase (EC 6.4.1.2), differentially accumulated. The results also showed that the accumulation of acyl-carrier-protein (EC 1.14.19.2), which is related to fatty acid biosynthesis, was up-regulated in CS compared with NS. Moreover, the fatty acid degradation-related proteins acetyl-CoA acyltransferase (EC 2.3.1.16), acetyl-CoA C-acetyltransferase (EC 2.3.1.9) and enoyl-CoA hydratase (EC 4.2.1.17) was up-regulated in both CS compared with NS and GS compared with CS. Glycerate dehydrogenase (EC 1.1.1.29), glycine hydroxymethyl transferase (EC 2.1.2.1), ribulose-bisphosphate carboxylase large chain (EC 4.1.1.39) and isocitrate lyase (EC 4.1.3.1) are associated with glyoxylic acid and dicarboxylic acid metabolism, and their accumulation was up-regulated in GS compared with CS. Starch and crude fat are degraded and converted into soluble sugars and other small molecular substances used for *H. moellendorffii* seed growth and embryo development. Fig. 6 shows a proposed model of the involvement of carbon metabolism in *H. moellendorffii* seed germination on the basis of our protein accumulation results.

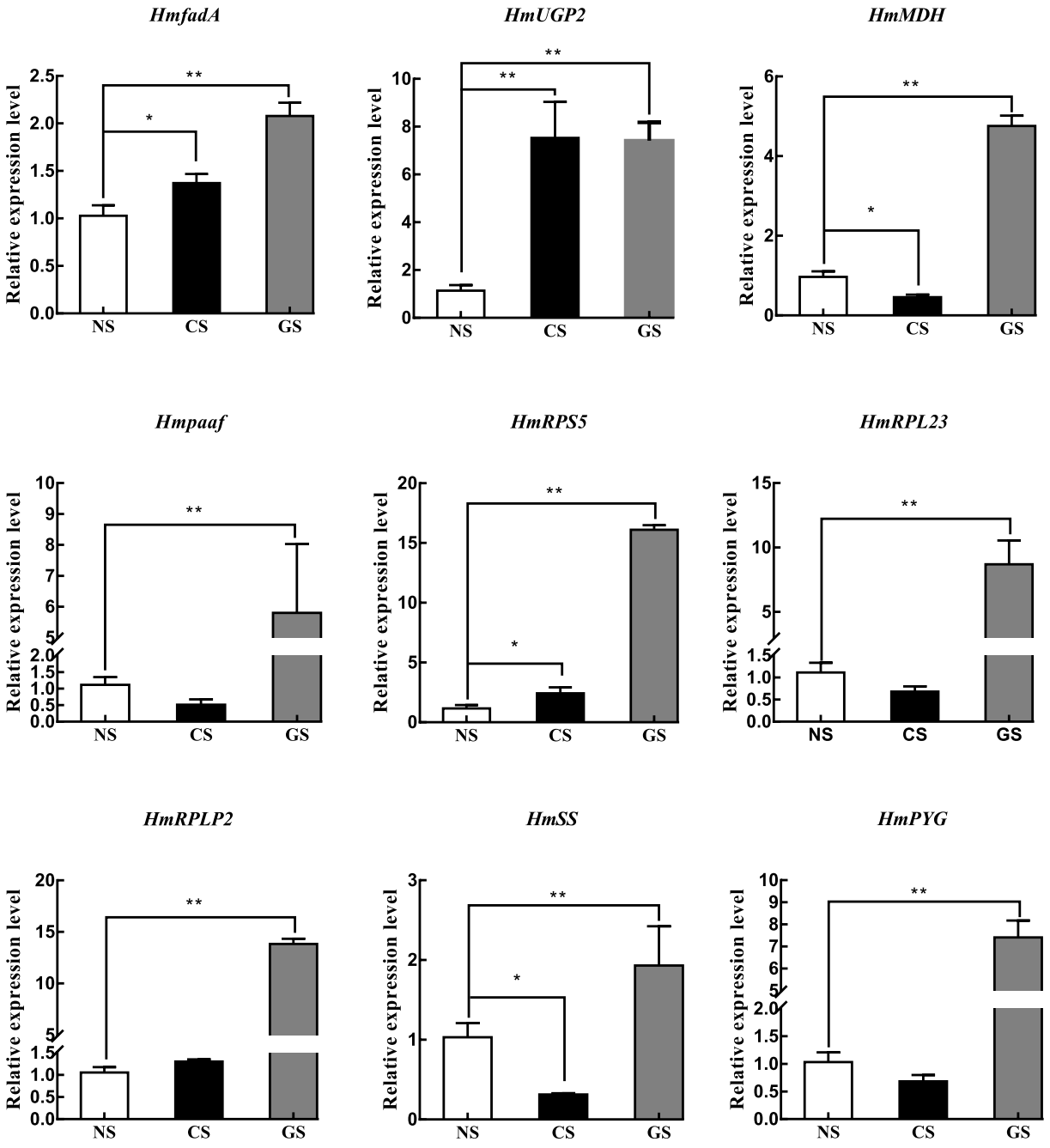

Fig. 7. qRT-PCR validation of different protein-coding genes, including acetyl-CoA acyltransferase (fadA, EC 2.3.1.16), UTP-glucose-1-phosphate uridylyl transferase (UGP2, EC 2.7.7.9), malate dehydrogenase (MDH, EC 1.1.1.37), enoyl-CoA hydratase (paaF, EC 4.2.1.17), 40S ribosomal protein S5 (RPS5), 60S ribosomal protein L23 (RPL23), 60S acidic ribosomal protein P2 (RPLP2), sucrose synthase (SS, EC 2.3.1.16), and glycogen phosphorylase (PYG). One-way analysis of variance (ANOVA) of data from cotyledon-stage-embryo seeds (CS) and germinated seeds (GS) compared with non-stratified seeds (NS). The asterisks indicate statistical significance, *P < 0.05, **P < 0.01. The error bars represent the means ± SEMs.

3.6. qRT-PCR analysis of differentially accumulated proteins

Stored substances play an important role in seed germination. It was found that these differentially accumulated proteins were significantly enriched in carbohydrate, fatty acid and protein metabolism-related pathways according to GO and KEGG analyses. Fourteen ribosomal proteins were identified in CS compared with NS, and 33 ribosomal proteins were identified in GS compared with NS (Supplementary Table 5). Differentially accumulated proteins from the above pathways, including PYG, UGP2, MDH, fadA, paaF, SS, 40S ribosomal protein S5 (RPS5), 60S ribosomal protein L23 (RPL23) and 60S acidic ribosomal protein P2 (RPLP2), were selected to obtain their corresponding gene sequence for qRT-PCR verification. The results showed that, with the exception of that of *HmUGP2*, the expression trend of the protein-coding genes was consistent with that of the protein accumulation in GS compared with NS. Moreover, compared with those in NS, the expression trends of *HmMDH*, *HmpaaF* and *HmRPL23* in GS were consistent with their changes in protein accumulation. Gene expression exhibits spatiotemporal specificity, which causes differences between the expression of several protein-coding genes and the accumulation of their proteins (Fig. 7).

4. Discussion

4.1. Carbohydrate metabolism during seed germination

Carbohydrate metabolism is ubiquitous during seed germination (Finch-Savage and LeubnerMetzger, 2006). The activation of carbohydrate metabolism during seed germination has been detected in many higher plant species (Liu, 2015). The results showed that the accumulation of proteins involved in starch synthesis was up-regulated in the early stage but down-regulated in the late stage during 4 °C stratification of *H. moellendorffii* seeds. The results also showed that the synthesis of starch diminishes during stratification of *H. moellendorffii* seeds. Up-regulated accumulation of enzymes involved in starch catabolism indicates involvement in the forward progress of the EMP. The accumulation of xylose isomerase was also shown to be up-regulated during the germination of rice (Xu and Cai, 2010). In the present study, the accumulation of xylose isomerase was up-regulated in the early stage of stratification, but it decreased in the late stage, indicating that the EMP is an important pathway of seed respiration during embryo development. The accumulation of other proteases located involved in the EMP and TCA were up-regulated in GS compared with CS, indicating that the energy in the late stage of seed stratification was provided by the EMP and TCA. Fluctuations in the accumulation of energy metabolism-related proteins were also revealed via grassbur germination proteomic analysis (Zhang et al., 2016). PYG, MDH and SS were also detected during stratification, and the expression trend of these protein-coding genes was the same as the protein accumulation trend in both GS and NS. However, the accumulation of PYG and SS differed from the expression of their coding genes. We speculate that this difference was due to the temporal and spatial specificity of gene expression.

The conversion of fats into carbohydrates during seed germination is achieved by the glyoxylate cycle and has been reported in oil seeds such as peanuts (Wang et al., 2016). In this study, the differentially accumulated proteins associated with fatty acid degradation did not change significantly in the early stage but were up-regulated in the late stage. It is inferred that, during seed dormancy release, the proteins associated with fatty acid degradation are activated. FadA and paaF were detected during stratification, and the expression trend of these coding genes was the same as the protein accumulation trend. Moreover, the degradation of lipids provides energy and substances for seed germination. Dynamic changes in the accumulation of proteins associated with fat metabolism therefore have an effect on seed dormancy and germination processes.

The results of this study showed that many differentially accumulated proteins associated with carbohydrate metabolism was not significant in CS compared with NS but was significant in GS compared with CS. It is thus important to study the dormancy and germination mechanisms of *H. moellendorff*i seeds in the future.

4.2. Protein degradation and biosynthesis during seed germination

A series of proteins related to protein degradation and biosynthesis were detected during *H. moellendorffii* seed germination, among which ribosome biosynthetic proteins accounted for a large proportion. Ribosomes are the main site of protein biosynthesis. The result of this study showed that, compared with that in NS, the accumulation of ribosomal proteins in the GS was up-regulated, and the expression trend of the coding gene was the same as the protein accumulation trend. In plants, eukaryotic translation initiation factor 5A (eIF5A) is involved in cell division; this protein promotes the activation of intracellular RNA polymerase and initiates mRNA transcription (Hopkins et al., 2008). In addition, eIF5A participates in protein biosynthesis to maintain cell wall and Actin integrity (Thompson et al., 2004). The results of this study showed that the accumulation of eIF5A was significantly down-regulated in GS compared with CS, which was consistent with the differential accumulation of this protein during the dormancy of potato tubers (Finch-Savage and Leubner-Metzger, 2006). The results of this study also showed that the accumulation of eEF1-β, which is associated with protein biosynthesis, was up-regulated and that the accumulation of Actin was down-regulated in GS compared with CS. eEF1-β is involved in transporting translated mRNA to the cytoplasm and is closely related to cell division. Actin filaments form an essential part of all eukaryotic cytoskeletons (Pajares and Pérez-Sala, 2006). In plants, Actin plays a role in basic activities such as cytoplasmic flow, organelle orientation and tip growth (Orvar et al., 2010). In addition, proteins are hydrolyzed into amino acids under acid-base conditions by enzymes. The amino acids in the final product are then hydrolyzed to participate in multiple biological processes. This study identified three differentially accumulated proteins associated with protein degradation. Moreover, homocysteine methyltransferase is a catalytic enzyme belonging to the transferase family, and it can transfer a methyl group containing a carbon group and participates in the metabolism of glycine, serine, threonine and methionine (Balbuena et al., 2011). Research has shown that homocysteine methyltransferase can also bind to tubulin (Finkelstein et al., 2008). In addition, homocysteine methyltransferase is capable of regulating apolipoprotein expression, resulting in increased levels of associated lipoproteins and stimulating and enhancing biofilm activity. The proteasome is a catalytic protease complex that removes misfolded or damaged proteins and controls the levels of certain regulatory proteins (Hai et al., 2015). Aspartic protease plays an important role in plant metabolism (Park et al., 1994). This study found that homocysteine methyltransferase was up-regulated in GS compared with CS. The accumulation of proteasome and aspartic protease were down-regulated in GS compared with CS. The content of soluble protein in *H. moellendorffii* seeds decreased during dormancy release. Overall, protein hydrolysis during stratification was the overall trend during *H. moellendorffii* seed germination, which lays a foundation for seed germination.

4.3. Stress responses and redox regulatory proteins during seed germination

In this proteomic analysis, we observed many differentially accumulated proteins related to the stress response among NS, CS and GS. Late-embryogenesis abundant (LEA) proteins comprise a class of proteins that highly accumulate during seed maturation. The accumulation of LEA is also induced when plants are subjected to drought and freezing stresses, and plants have enhanced dehydration tolerance under adverse conditions to ensure cell viability. In this study, differential accumulation of LEAs was not detected in CS compared with NS, and LEAs were down-regulated in GS compared with CS. LEAs were shown to be gradually degraded during oat seed germination (Leal and Misra, 1993). LEA degradation in the early stage of germination plays an important role in activating metabolism. Heat shock proteins (HSP) play a crucial role in protecting plants from stress, and the role of small-molecular weight-heat shock protein (sHSP) in the development of pea seeds has been identified (Wehmeyer et al., 1996). Developmentally dependent sHSPs were also identified in wheat seed embryos and were closely related to seed desiccation resistance, embryo development, dormancy, and germination (Helm and Abernethy, 1990). HSP70, HSP90-6, HSP80 and HSP83 were identified during the stratification of *H. moellendorffii* seeds. Among them, HSP70 has been researched the most in animal and plant embryos. HSP70 has molecular chaperone and antiapoptotic functions, which could promote embryo development. HSP90 plays a role in seed development and embryogenesis (Wehmeyer et al., 1996). In this study, the accumulation of HSP 70 was up-regulated in CS compared with NS but was downregulated in GS compared with CS. The content of HSPI did not change between CS and NS but was down-regulated in GS than in CS.

During dormancy release and germination, seeds produce a large amount of reactive oxygen species (ROS) and hydrogen peroxide (H2O2). These ROS directly or indirectly initiate membrane lipid peroxidation, damaging cell membrane structure and membrane

permeability (Ying et al., 2006). Antioxidant enzymes such as POD, CAT, SOD and APX are mainly involved in limiting ROS and H2O2. Antioxidant processes have been observed during the germination of *Davidia involucrate* seeds (Yang et al., 2015). The results of this study showed that the HSP of APX was down-regulated during germination. In addition, CAT and SOD showed differential abundance during *H. moellendorffii* seed germination. In addition, the activity of various antioxidant enzymes during buckwheat seed germination indicated that the seeds produced ROS and that free radicals activated antioxidant enzymes (Desen and Al, 2003). Dormancy is the result of the long-term evolution of seeds and has allowed them to adapt to environmental stress. On the basis of the above analysis, it can be inferred that the accumulation of antioxidant enzymes reflects the dormancy degree of *H. moellendorffii* seeds.

H. moellendorffii seeds exhibit morphological post-ripening characteristics. The embryo is heart shaped in NS and is surrounded by the endosperm at the low end of the seed, and the cotyledons and radicles are not fully developed. This phenomenon is quite different from other non-dormant seeds internal structures. After the *H. moellendorffii* seeds were treated with the 4 °C stratification treatment, the embryos were elongated, the cotyledons unfolded, the cotyledons clearly thickened, and the heart-shaped embryos gradually developed into cotyledon-stage embryos. The embryonic development of *Changium smyrnioides* is similar to that observed in this study (Qiu, 2001). The main activities of the endosperm during this period are the activation of various metabolic systems and the mobilization of stored substances within the seeds (Zhang and Jing, 2015). The length of the embryos did not significantly change in the period after the cotyledon-stage embryos formed, but at the end of this stage, the seeds had germinated. Moreover, the physiological and biochemical indexes of the NS, CS and GS significantly changed, and the contents of soluble sugars, soluble starch, soluble protein and crude fat (stored substances) continued to decline over time. During seed germination, stored substances are decomposed so that their components are synthesized into new substances that participate in seed dormancy release. At the same time, the metabolic energy of these substances is used to divide blast cells in preparation for further differentiation of the radicle (Jm et al., 2014). When the energy for germination accumulates to a certain degree, the radicle penetrates the seed coat. There is a certain relationship between the growth status of embryos and nutrient metabolism. In the future, after analyzing a series of differentially accumulated proteins detected during the low-temperature stratification, we will further study the dormancy release of *H. moellendorffii* seeds.

5. Conclusion

Seed germination is a complex biological process that requires the coordination of both environmental and genetic factors. As the embryonic morphology of *H. moellendorffii* seeds develops, the contents of stored substances within the endosperm continuously decrease. The TMT technique was used to quantify the proteome of *H. moellendorffii* seeds at three critical stages of seed germination. The results showed that *H. moellendorffii* seed germination was accompanied by various metabolic processes to meet the energy and substrate needs of the seeds. The differentially accumulated proteins were significantly enriched in the pathways of pyruvate metabolism, fatty acid metabolism, starch and sucrose metabolism during germination, and the changes in stored contents confirmed these results. EIF5A, eEF1-β and Actin, which are related to protein biosynthesis and degradation, were found to regulate *H. moellendorffii* seed germination. Proteins related to stress responses and redox reactions, including Hsp, LEA and APX, were also differentially accumulated. These proteins differentially accumulate to allow the seeds to adapt to the germination environment. Overall, the process of seed germination was explored by studying stratified seeds at the morphological, physiological, and proteomic levels. The results of this study provide a theoretical basis for breaking *H. moellendorffii* seed dormancy.

Additional explanation

1. The seeds of *Heracleum moellendorffii* Hance have dormant property and the type of dormancy belong to the morphological physiological dormancy. Our research team found that low temperature stratification can relieve its dormancy and promote its germination. The stratification contains morphological ripening of seeds and the process of germination.

2. Microsurgical observation was carried out before stratification of *Heracleum moellendorffii* Hance seeds, it was found that its embryo was very small and in the heart-shaped embryo stage. Samples were taken continuously for anatomical observation during stratification. It was found that the morphology and size of embryos changed during stratification. The regularity of morphological change is as follows: Heart-shaped embryo, Torpedo shaped embryo, Cotyledon stage embryo, Germination. Comparisons of seed embryos in stratification are calculated by embryo rate, which increases during stratification.

3. Cotyledon stage embryo is a marker of the completion of morphological post-ripening in *Heracleum moellendorffii* Hance seeds. After that, the morphology of the embryo did not change, but it still took some time for the radicle to break through the seed coat. Therefore, we focus on the comparative analysis of proteomics among heart-shaped embryo seeds, cotyledon stage embryo seeds and germinated seeds.

4. The seeds for proteome analysis were non-stratified seeds, cotyledon stage embryo seeds and germinated seeds. Among them, non-stratified seeds corresponded to 0 days of 4°Cstratification, cotyledon stage embryo and germinated seeds corresponded to 90 and 150d of 4 °C stratification. These three periods are abbreviated by NS, CS and GS respectively.

5. Fig. 1 in the text shows the photography and size of embryos in three critical periods. Since the embryo rate of germinated seeds have reached 100%, it is not compared with other two stages by embryo rate and embryo morphology. Table 1 shows the basic information of seeds at three critical stages during 4 °C stratification.

Contribution

F. H. Li and P. Yu designed this work. P. Yu, C.H. Song and J. J. Wu collected the samples, analyzed the samples. F. H. Li, P. Yu, C.H. Song drafted the manuscript. P. Yu, C.H. Song and Y. Tian performed parts of the experiments in the laboratory. X. F. Wu, X. W. Zhang and Y. M. Liu revised the manuscript. All authors have read and approved the final manuscript.

Declaration of competing interest

The authors declare that they have no conflict of interest.

Acknowledgments

This study was funded by the National “Thirteenth Five-Year” Key Research and Development Program of China (2016YFC0500307). We are grateful to the Forest Botanical Garden of Heilongjiang Province for supplying the seeds of *H. moellendorffii* Hance. We would like to thank all professors in the Plant Physiology and Molecular Biology lab for revising the manuscript. We also would like to acknowledge Beijing Protein Innovation for their helpful suggestions concerning the data analysis.

Appendix A. Supplementary data

Supplementary data to this article can be found online at https://doi.org/10.1016/j.plaphy.2019.10.002.

References

Balbuena, T.S., Jo, L., Pieruzzi, F.P., Dias, L.L.C., Silveira, V., Santa-Catarina, C., 2011. Differential proteome analysis of mature and germinated embryos of Araucaria angustifolia. Phytochemistry 72, 302–311.

Bao, J.P., Zhang, S.L., 2011. Changes in germination, storage materials and antioxidant enzyme activities in pear (Pyrus betulaefolia Bge. and Pyrus calleryana Dcne.) stock seeds during cold stratification. Seed Sci. Technol. 39, 655–659.

Campos, M.D., Frederico, A.M., Nothnagel, T., Arnholdt-Schmitt, B., Cardoso, H., 2015. Selection of suitable reference genes for reverse transcription quantitative real-time pcr studies on different experimental systems from carrot (daucus carota l.). Sci. Hortic. 186, 115–123.

Chung, S.L., Ching, T.C., Chao, H.L., Yi, Y.C., Yuh, S.Y., 2010. Protein changes between dormant and dormancy-broken seeds of Prunus campanulata Maxim. Proteomics 6, 4147–4154.

Desen, K.E., Al, E., 2003. Relationship between ascorbic acid and germination of seeds. Chin. J. Appl. Environ. Biol. 9, 513–516.

Diao, S., Zhu, N., Sun, G., 2010. Nutrients and processing characteristics of spuriopimpinella brachycarpa. J. Northeast For. Univ. 38, 48–50.

Finch-Savage, W.E., Leubner-Metzger, G., 2006. Seed dormancy and the control of germination. New Phytol. 171, 501–523.

Finkelstein, R., Reeves, W., Ariizumi, T., Steber, C., 2008. Molecular aspects of seed dormancy. Annu. Rev. Plant Biol. 59, 387–415.

Hai, L., Leng, Y.F., Zhou, S.F., Jian, L., Rong, T.Z., 2015. Proteomic analysis of storage substances during after-ripening of dormant seeds with dry ripening process in maize inbred line. J. Plant Genet. Resour. 16 (26), 23–28.

Helm, K.W., Abernethy, R.H., 1990. Heat shock proteins and their mRNAs in dry and early imbibing embryos of wheat. Plant Physiol. 93, 1626–1633.

Hopkins, M.T., Yulia, L., Tzann, W.W., Zhongda, L., Thompson, J.E., 2008. Eukaryotic translation initiation factor 5A is involved in pathogen-induced cell death and development of disease symptoms in Arabidopsis. Plant Physiol. 148, 479–489.

Jm, L.P.T., Lumaret, R., Flaven, N.E., Sauve, M., Dubois, M.P., Danthu, P., 2014. Nuclear microsatellitevariation in Malagasy baobabs (Adansonia, Bombacoideae, Malvaceae) reveals past hybridizationand introgression. Ann. Bot. 112, 796–807.

Leal, I., Misra, S., 1993. Developmental gene expression in conifer embryogenesis and germination. III. Analysis of crystalloid protein mRNAs and desiccation protein mRNAs in the developing embryo and megagametophyte of white spruce (Picea glauca (Moench) Voss). Plant Sci. 88, 25–37.

Laurentin, A., Edwards, C.A., 2003. A microtiter medication of the anthrone sulfuric acid colorimetric assay for glucose-based carbohydrates[J]. Anal. Biochem. 315 (1), 143–145.

Li, M.Y., Wang, F., Jiang, Q., Wang, G.L., Tian, C., Xiong, A.S., 2016. Validation and comparison of reference genes for qPCR normalization of celery (Apium graveolens) at different development stages. Front. Plant Sci. 7, 20–21.

Li, F.H., Li, N.D., Liu, Z.B., Cui Wei, J.Q., Yu, P., Xu, Q.H., 2017b. Study on *Heracleum moellendorffii* Hance seed morphology after ripening during different stratification condition. J. Northeast Agric. Univ. 48, 28–34.

Li, F.H., Liu, Z.B., Cui Wei, J.Q., Yu, P., Lv, Y., Xu, Q.H., 2017a. Growth and development rule and correlation analysis of main characters of *Heracleum moellendorffii* Hance. J. Northeast Agric. Univ. 48, 15–22.

Liu, B., et al., 2015. Proteomic changes during tuber dormancy release process revealed by iTRAQ quantitative proteomics in potato. Plant Physiol. Biochem. 86, 181–190 2014.12.003.

Liu, S., Jiang, X., Liu, Z., Cheng, Y., Sun, T., Yu, X., 2018. Mechanism of the breaking of seed dormancy by flower thinning in Heracleum moellendorffii hance. J. Plant Growth Regul. 33, 73–84.

Lu, X.J., Zhang, X.L., Mei, M., Liu, G.L., Ma, B.B., 2016. Proteomic analysis of Magnolia sieboldii K. Koch seed germination. Journal of Proteomics 133, 76–85.

Orvar, B.L., Sangwan, V., Omann, F., Dhindsa, R.S., 2010. Early steps in cold sensing by plant cells the role of actin cytoskeleton and membrane fluidity. Plant J. 23, 785–794.

Pajares, M.A., Pérez, S.D., 2006. Betaine homocysteine S-methyltransferase just a regulator of homocysteine metabolism? Cell. Mol. Life Sci. 63, 2792–2803.

Park, M.H., Wolff, E.C., Lee, Y.B., Folk, J.E., 1994. Antiproliferative effects of inhibitors of deoxyhypusine synthase. Inhibition of growth of Chinese hamster ovary cells by guanyl diamines. J. Biol. Chem. 269, 27827.

Pawłowski, T.A., Staszak, A.M., 2016. Analysis of the embryo proteome of sycamore (Acer pseudoplatanus L.) seeds reveals a distinct class of proteins regulating dormancy release. J. Plant Physiol. 195, 9–22.

Qiu, Y.X., 2001. Studies on the endangerment mechanism of and conservation strategies for Changium smyrnioides. Chin. Biodivers. 3, 70–71.

Simpson, R.J., Dorow, D.S., 2001. Cancer proteomics, from signaling networks to tumor markers. Trends Biotechnol. 19, 40–48.

Tang, Z.Y., 1999. Modern Plant Physiology Experiment Guide.

Thompson, J.E., Hopkins, M.T., Catherine, T., Tzann, W.W., 2004. Regulation of senescence by eukaryotic translation initiation factor 5A implications for plant growth and development. Trends Plant Sci. 9, 174–179.

Wang, Y., Ma, X., Zhang, X., He, X., Li, H., Cui, D., Yin, D., 2016. ITRAQ-based proteomic analysis of the metabolic mechanisms behind lipid accumulation and degradation during peanut seed development and post germination. J. Proteome Res. 15, 4277–4289.

Wang, J.H., Yu, X.H., Jiang, X.M., 2017. Comparative analysis to different ecological conditions on main growth period and nutritional components of *Heraclenm* dissectum. China Cucurbits Veg. 30, 14–17.

Wehmeyer, N., Hernandez, L.D., Finkelstein, R.R., Vierling, E., 1996. Synthesis of small heat-shock proteins is part of the developmental program of late seed maturation. Plant Physiol. 112, 747–757.

Wijayabandara, S., Jayasuriya, K., Jayasinghe, J., 2013. Seed dormancy, storage behavior and germination of an exotic invasive species Lantana camara L (Verbenaceae). Int. Res. J. Biol. Sci. 2, 7–14.

Wu, Z.Y., Raven, P., 1994. Flora of China[M]. Science Press.

Xu, L., Cai, J., 2010. Differential proteomic and mass spectrometric analysis of embryo buds during seed germination in rice (oryza sativa L.). Chinese Agricultural Science Bulletin 26, 10–16.

Yang, L., Shen, H.L., Liang, L.D., 2008. Changes in endogenous hormone content in seeds of sorbus pohuashanensis (hance) hedl during artificial drying and cold stratification. Plant Physiol. Commun. 44, 682–688.

Yang, Y., Yun-Xiang, L.I., Xiao, X.U., 2015. The activity of principal antioxidant enzymes and the content of metabolites in dormancy breaking and germination of davidia involucrate seeds. Plant Diversity & Resources 33, 779–787.

Ying, R., Liu, K., Lin, S., Tian, H., Sheng, J.P., 2006. Metabolism of dynamic changes of the reactive oxygen in tomato pericarp and seed tissues during fruit ripening and senescence. Acta Hortic. Sin. 33, 63–67.

Zhang, G., Jing, H.U., 2015. Changes of the storage substances and enzyme activity of Chionanthus retusus seeds during alternative stratification. China Forestry Science & Technology 29, 24–27.

Zhang, G.L., Zhu, Y., Fu, W.D., Wang, P., Zhan, R.H., Zhang, Y.L., 2016. iTRAQ protein profile differential analysis of dormant and germinated grassbur twin seeds reveals that ribosomal synthesis and carbohydrate metabolism promote germination possibly through the PI3K pathway. Plant Cell Physiol. 57, 1244–1256.